ANNALS OF GEOPHYSICS, 66, 3-4, SE320, 2023; doi:10.4401/ag-8974
OPEN ACCESS

Recent seismicity in the Messina area, southern Italy, and comparison to the local geology and tectonics

Giancarlo Neri[*,1], Barbara Orecchio[1], Paolo Pino[1,2], Debora Presti[1], Silvia Scolaro[1,2] and Antonino Torre[1,2]

(1) Department of Mathematics, Computer Sciences, Physics, and Earth Sciences, University of Messina
(2) Department of Engineering, University of Messina

Article history: received April 24, 2023; accepted July 5, 2023

Abstract

We have investigated the seismicity occurred during 2000-2021 in the area of Messina, the town which suffered greatest loss of human lives over the territory devastated by the magnitude 7.1 earthquake of December 28, 1908. We have found that most of recent activity was located beneath the historical centre of the town, in and near the very peculiar sickle-shaped harbor zone which prompted the Greek colonizers in the VII Century B.C. to give Messina the old name of "Zancle" ("Sickle" in the ancient Greek language). Extracting from the whole dataset (consisting of hundred earthquakes of maximum magnitude 3.8) the data relative to a small sequence of 28 events concentrated in a few days at the end of 2013, and performing high-quality Bayesian hypocenter locations of these events, we have found very clear epi-hypocentral trends suitable for comparison with the local structural scenario. The joint analysis of seismic, geological and geomorphological data including morphobathymetric curves of the sea bottom in the study area, has brought us to propose that the small sequence in question (and probably most of activity recorded during the whole 22-years period) may have been generated by internal dynamics of a local horst/graben system, the position of which (i) appears to correspond to one of the minor horsts documented in the Messina Strait basin area and (ii) is very close to the upper edge of the 1908 earthquake blind source reported in the Database of Individual Seismogenic Sources of the Italian National Institute of Geophysics and Volcanology.

Keywords: Earthquake location; Faults; Bathymetric data; Local tectonics; Messina Strait

1. Introduction

In Italy and Europe, the town of Messina (Figure 1) is paradigmatic of seismic risk, mainly due to the major earthquake of 28 December 1908 which caused about 80000 victims in the city and over the whole territory around the Messina Strait [Guidoboni et al., 2019]. As the main town of this territory, Messina suffered greatest devastation from this magnitude 7.1 earthquake in terms of human lives and damage to buildings and infrastructures.

Many geological and geophysical studies have been performed in this area over the last 50 years, with the primary goals of understanding the local geodynamics and identifying the source of the 1908 earthquake. Concerning the 1908 earthquake source, although the debate does not appear to be still concluded [e.g., Meschis et al., 2019; DISS Working Group, 2021; Barreca et al., 2021; Pino et al., 2021; Argnani, 2022; Argnani and Pino, 2023], we may register today a substantial convergence of scientists toward an east-dipping, circa NNE-striking normal fault with top located near the Sicilian shoreline of the Strait, with moderate differences among the different investigators concerning (i) the angles of fault dip and strike and (ii) the location of the upper edge of the source.

At the same time, the literature shows that the recent seismicity of the same area has, to date, received quite limited attention by the scientific community [Bottari et al., 1989; Neri et al., 2004 and 2021; Scarfì et al., 2016]. This was basically due to two reasons: (i) marked improvement of the seismic monitoring system was realized only in the late 1990s [Amato and Mele, 2008; Schorlemmer et al., 2010] and (ii) low levels of seismicity have been recorded in

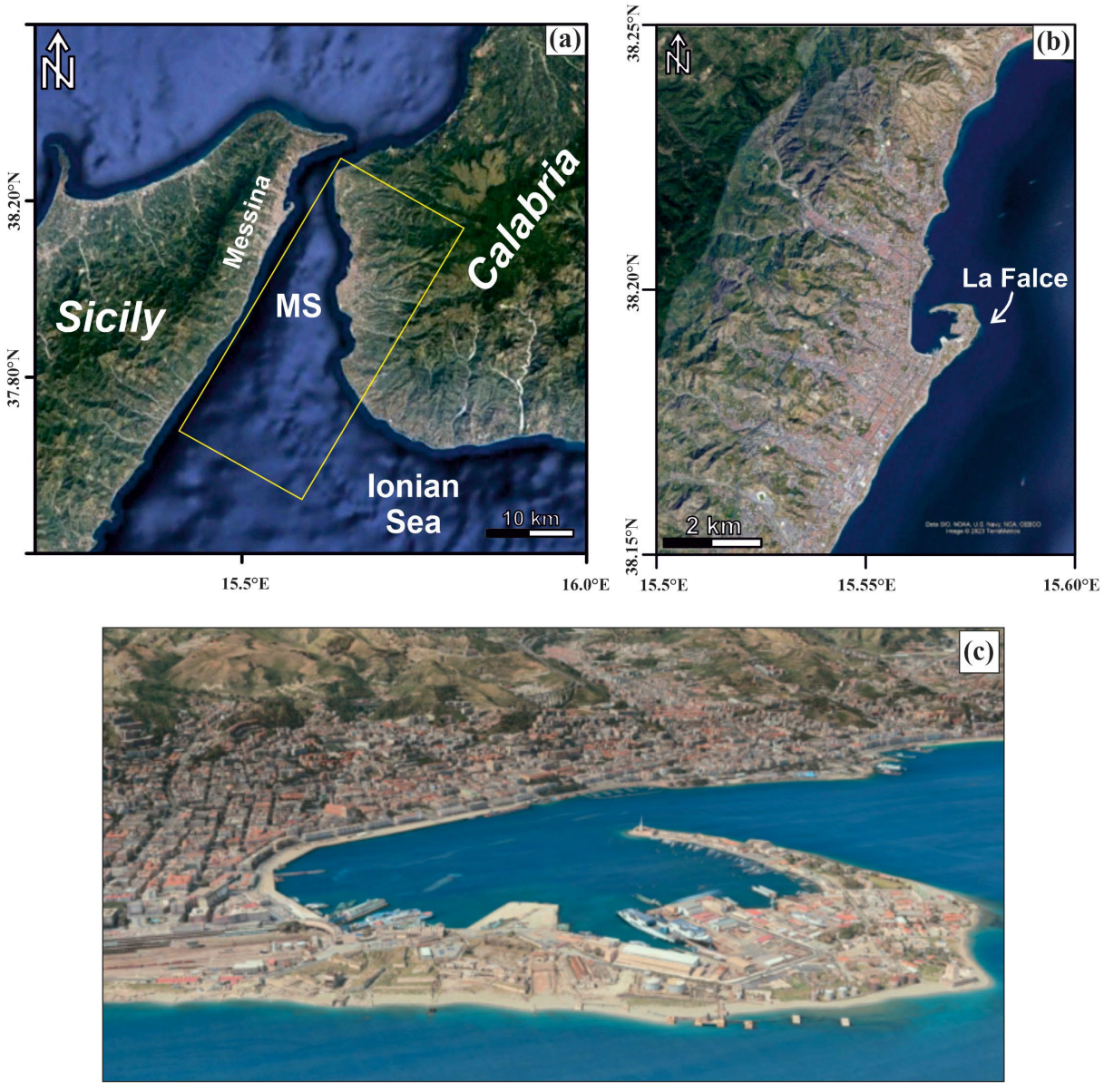

Figure 1. (a) Satellite image of the Messina Strait area and surroundings from Google Earth Pro 2022. The yellow rectangle indicates the surface projection of the SE-dipping blind normal fault reported in the Database of Individual Seismogenic Sources of the National Institute of Geophysics and Volcanology of Italy (DISS Working Group, 2021) as the source of the magnitude 7.1 earthquake of 28 December 1908. (b) Satellite image of Messina city with the peculiar sickle-shaped natural structure called *La Falce*. (c) Aerial sight of Messina city with *La Falce* in the foreground.

the last decades (Figure 2). As a result, a 20yrs-long good-quality database is today available, although inevitably limited to low-magnitude earthquakes. On the whole, it can be stated that a fairly low seismic activity affected the area of the town of Messina over a time span of ca. 70 years (i.e. since 1950), basically consisting of an earthquake of magnitude 4.7 and a few earthquakes of magnitude 3.5-4 [Bottari et al., 1989; http://terremoti.ingv.it/, ISIDe Working Group, 2007].

In the present study we investigate the seismicity shallower than 20 km occurring during 2000-2021 in the Messina area (Figure 1). From a preliminary analysis of the Italian national seismic bulletin (http://terremoti.ingv.it/, ISIDe Working Group, 2007) we have noted that most of the 2000-2021 seismicity of this area occurred in correspondence of (or close to) a peculiar geological feature of the town, having also a relevant historical and landscaped value (Figure 2). The feature in question is named *La Falce* (Italian translation of "The Sickle") and represents a clear irregularity of the otherwise nearly linear shape of the Sicilian coast of the Messina Strait (Figure 1). From the geological point of view (see the forthcoming sections), "The Sickle" corresponds to a horst in the horst-and-graben structure of the Messina Strait area. It gives a quite impressive and beautiful look to the local landscape which, among other things, prompted the Greek colonizers to give Messina the old name of "Zancle" ("The Sickle" in the ancient Greek language) in the VII Century B.C.. In the long history of Messina, *La Falce* has always been the site of the main harbor of the town. *La Falce* and the Sicilian shoreline of the Messina Strait are close to the upper edge of the 1908 earthquake source as reported in the Database of Individual Seismogenic Sources of the Italian National Institute of Geophysics and Volcanology [Figure 1; DISS Working Group, 2021]. The 1908 earthquake caused diffused ground subsidence phenomena and great damage to local settlements in the *La Falce* area [Baratta, 1910; Guidoboni et al., 2018 and 2019]. The combined action by earthquake ground shaking and tsunami wave which inundated all the *La Falce* area a few minutes after the earthquake resulted devastating for industrial and military settlements which substantially represented the only kind of buildings in the *La Falce* area at the time of the earthquake [Baratta, 1910; Guidoboni et al., 2018 and 2019].

For our analysis of low-magnitude recent seismicity of the Messina area, we take benefit from (i) the good-quality seismic database of the last two decades [http://terremoti.ingv.it/, ISIDe Working Group, 2007; Amato and

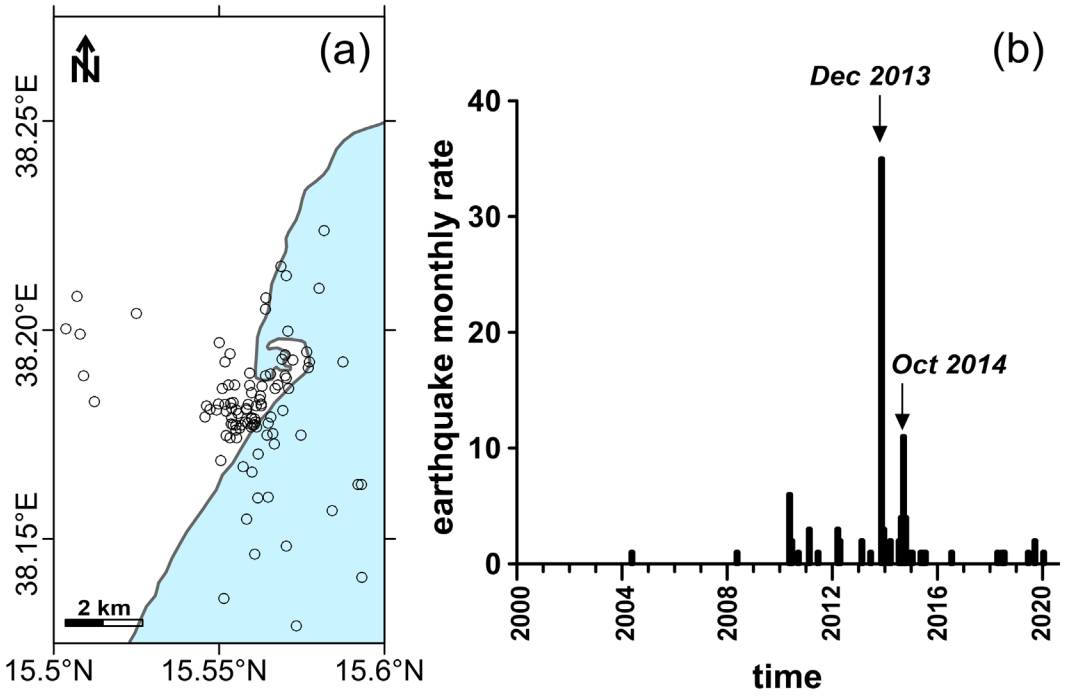

Figure 2. Plot (a) displays the epicentral map of earthquakes of magnitude over 1.0 that occurred between 2000 and 2021 at depths less than 20 km in the study area according to the Italian seismological database (http://terremoti.ingv.it/, ISIDe Working Group, 2007). Plot (b) reports the earthquake monthly rate for the same dataset shown in the map. The temporal pattern of the seismic occurrence rate highlights a clear peak of activity in December 2013 (35 events were concentrated between 23 and 28 December) and a minor peak in October 2014 emerging from the relatively high level of background activity of the same year.

Mele, 2008; Michelini et al., 2016], (ii) the recent methodological progresses in seismic data elaboration [e.g., Presti et al., 2008; D'Amico et al., 2011; Görgün and Albora, 2017; Görgün et al., 2020], and (iii) the joint analysis of seismic, geological and geomorphological data, which are in part released by the present study and in part taken from the literature.

2. Geological framework of the Messina area

The city of Messina is located within an important tectonic basin, the Messina Strait, shaped by normal faults mainly oriented NNE-SSW and ENE-WSW (Figure 3), which divides the southern Apennines from the Sicilian-Maghrebian Chain [Lentini et al., 1995, 2000]. Calabria and Northeast Sicily (i.e., the 'Calabro-Peloritan Arc', Figure 3) represent uplifted segments of an orogenic thrust belt [Ghisetti, 1981; Ghisetti and Vezzani, 1982; Finetti and Del Ben, 1986; Dewey et al., 1989; Lentini et al., 1994, 1995; Finetti et al., 1996] built up during Eocene to early-middle Miocene collisional phases. The orogenic belt, mainly made up of crystalline thrusted units covered by a post-collisional Late Miocene-Plio-Pleistocene sedimentary succession, displays the effects of intense Quaternary tectonics represented by regional uplift and extensional processes [Westaway, 1993; Billi et al., 2010; Faccenna et al., 2011; Monaco et al., 2017]. In the Messina Strait area, major evidences of the last phases of uplifting are the thick beds of Middle Pleistocene loose gravels and sands (Messina Fm.) and the different orders of middle-upper Pleistocene marine terracing, trasgressively covering the crystalline-methamorphic substratum, the Pliocene and the early Pleistocene sediments [Ghisetti, 1984]. In the same area, a complex and dense network of normal and transtensional faults [Doglioni et al., 2012] dissect the slopes of the Peloritani-Aspromonte orogen, bounding different horsts and half-graben structures (Figure 3). The local extensional dynamics are capable of strong earthquakes, such as the M 7.1 Messina earthquake of December 28, 1908 [Monaco and Tortorici, 2000; Neri et al., 2006 and 2020; Serpelloni et al., 2010]. In addition to the already mentioned main fault systems trending NNE-SSW and ENE-WSW, other diversely oriented fault systems (trending NNW-SSE, NW-SE and E-W) are documented both onshore and offshore in the Messina Strait area and are considered the result of a long-term geological history during which tectonic stress and strain have changed over time [Selli et al., 1978; Ghisetti, 1984 and 1992; Del Ben et al., 1996 and 2008; Lentini, 1999; Guarnieri et al., 2004]. All the fault systems seem to have participated simultaneously in the dynamics of the area at least until after the uppermost Pleistocene and it cannot be excluded that simultaneous action of the different fault systems is currently active [Selli, 1979; Guarnieri et al., 2004; Guarnieri and Pirrotta, 2008].

The inhabited centre of Messina is essentially built on Holocene coastal and alluvial deposits [Gargano, 1994; Bonfiglio et al., 1994; Lentini et al., 2000; Servizio Geologico d'Italia, 2008; Pino et al., 2023], covering a thick clastic loose formation named Messina Sands and Gravels (Middle Pleistocene). This formation makes up the hills to the west of the coastal plain (Figure 4), while still going west toward the more intensively uplifted Peloritani ridge (Figure 3) more ancient geological formations outcrop, in particular the Miocene siliciclastic succession of San Pier Niceto Fm. and the metamorphic substrate. Both the Peloritani ridge and the Sicilian coastline of the Strait (Figure 3) are oriented according to the aforementioned NNE-SSW and ENE-WSW structural systems, all reflecting the roughly NW-SE opening direction of the extensional tectonics of the area. A peculiar, and somewhat anomalous, feature in this context is *La Falce*, a sickle-shaped portion of the Messina city coastline that clearly interrupts the Ionian coastal linear trend (Figures 1 and 4). *La Falce* is a sort of appendix of the coastal plain, characterized by a flat landform few meters above sea level with geology represented by alluvial and coastal deposits (Figure 4). Some authors suggested the presence of a crystalline horst in the Messina city coastal area roughly in correspondence of *La Falce* [e.g. Baratta, 1910; Ghisetti, 1984; Guarnieri et al., 2004].

3. Data, analysis and results

3.1 Seismicity

Figure 2a shows that most of the shallow seismicity occurring in the Messina area during 2000-2021 is located beneath or near the *La Falce* geological structure. The maximum magnitude in the study area/period was relatively low (Ml 3.8) and all other earthquakes had magnitude not larger than 3.2. The temporal pattern of the seismic occurrence rate (Figure 2b) highlights a clear peak of activity in December 2013, corresponding to a small sequence of

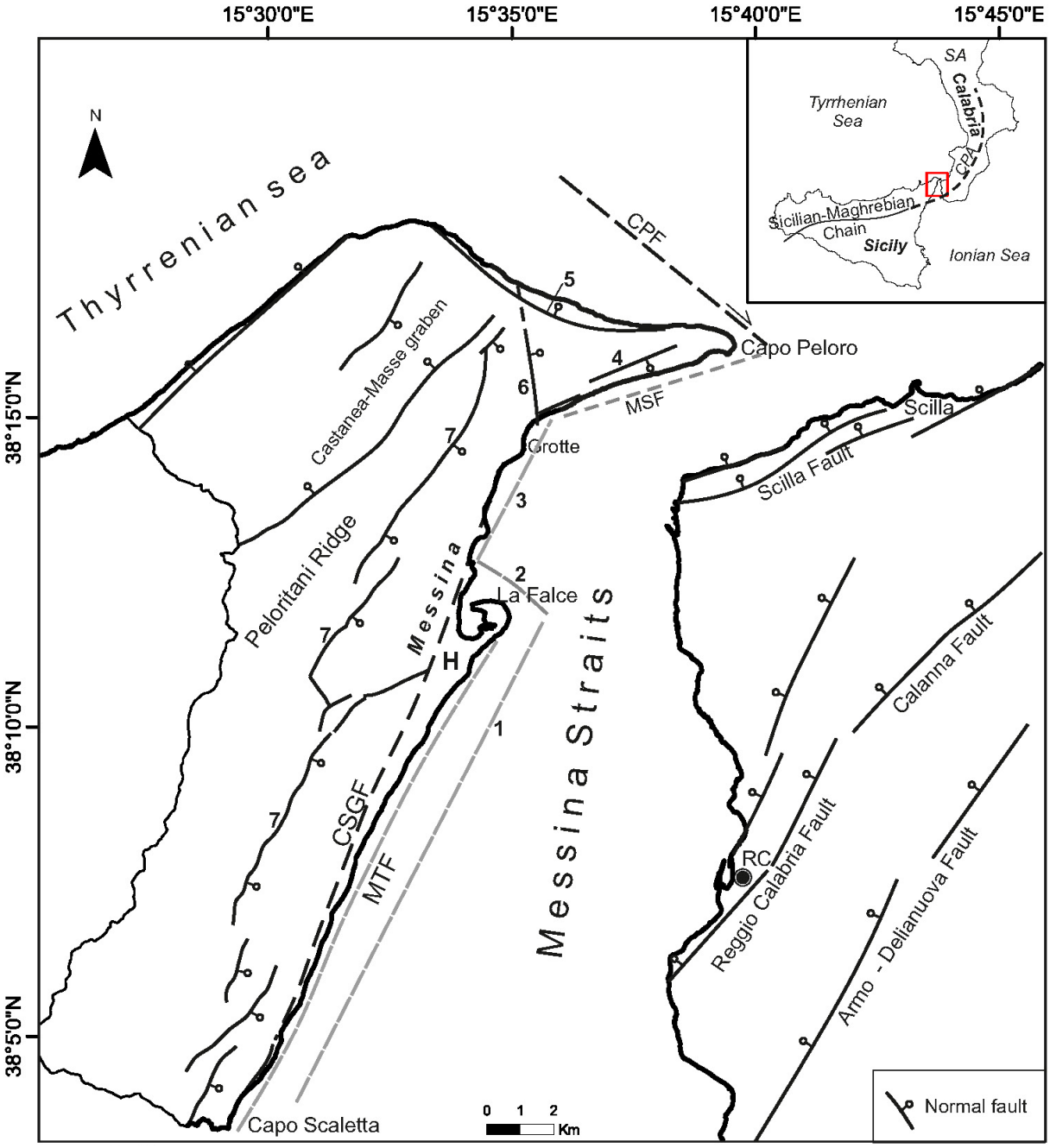

Figure 3. Simplified structural map of the Messina Strait area. Fault legend: CPF = Capo Peloro Fault [Doglioni et al., 2012]; MSF = Messina Strait Fault [Doglioni et al., 2012]; MTF = Messina-Taormina Fault [Dorsey et al., 2023]; CSGF = Capo Scaletta – Grotte Fault [Selli, 1979]; 1 from Del Ben et al. [2008]; 2 and 3 from Guarnieri et al. [2004]; 4= Granatari Fault [Ghisetti, 1992]; 5 = Mortelle Fault [Ghisetti, 1992]; 6 = Faro Superiore Fault [Guarnieri and Pirrotta, 2008]; 7 = Curcuraci-Larderia Fault System [Ghisetti, 1992]. Bibliographic sources of the faults on the Calabrian side are: Scilla Fault [Ferranti et al. 2008], Reggio Calabria Fault, Calanna Fault and Armo-Delianuova Fault [Ghisetti, 1992]. RC = Reggio Calabria city center. H stands for Messina horst [Ghisetti, 1984]. In the inset, the curved dashed line indicates the Calabro-Peloritan Arc (CPA); SA = Southern Appennines. The rectangle indicates the study area.

few tens of earthquakes which started with the magnitude 3.8 earthquake of 23 December 04:20 GMT and ended with the magnitude 1.4 earthquake of 28 December 16:05 GMT. In the Figure 2b, a minor peak can be noted in October 2014 emerging from the relatively high level of background activity of the same year, what leads us to suspect that seismic activity in 2014 may have been related to some extent to the sequence of December 2013.

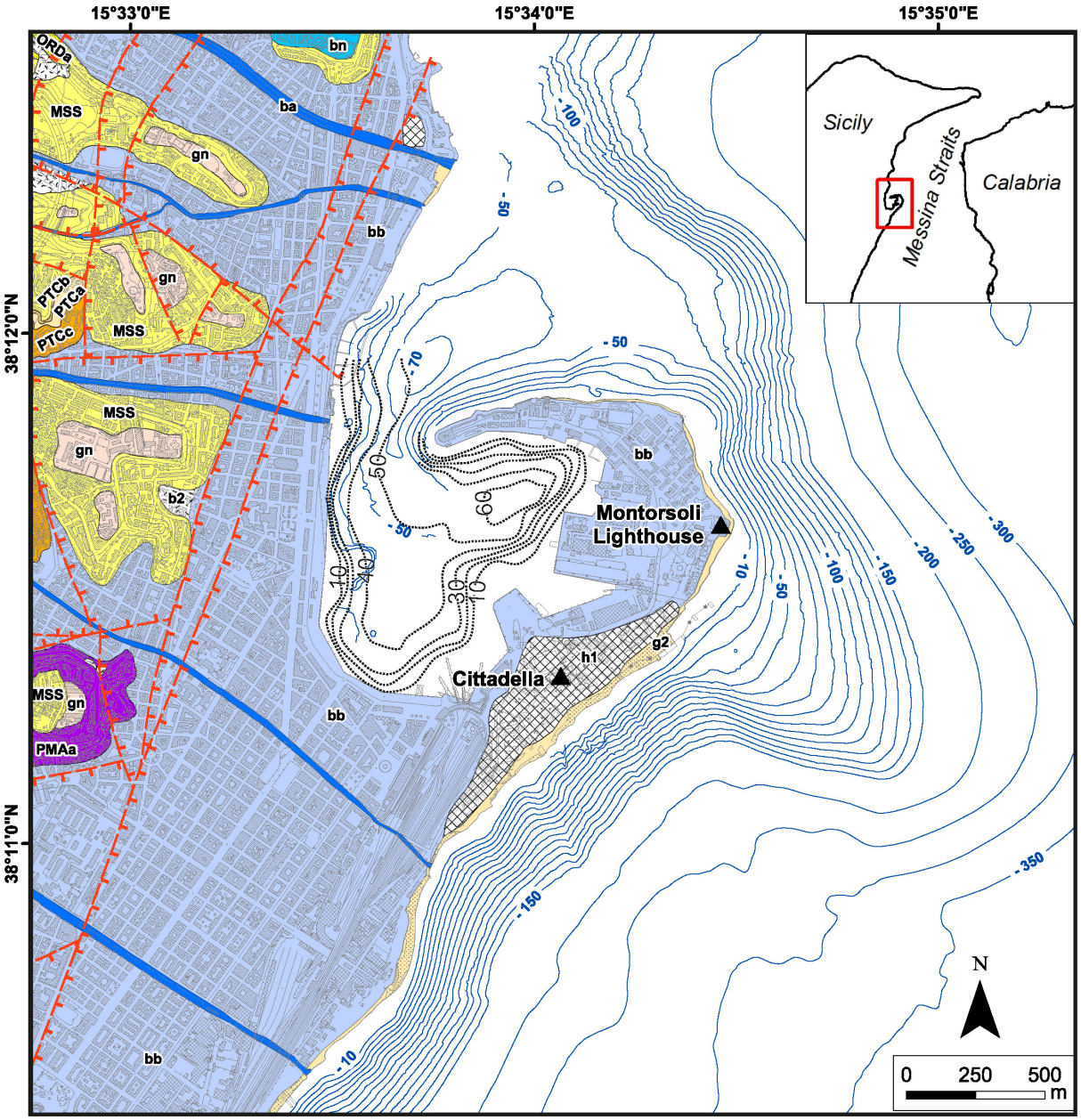

Figure 4. Geological map of *La Falce* and surroundings in Messina city [from Gargano, 1994; Lentini et al., 2000; Servizio Geologico d'Italia, 2008; modified from Pino et al., 2023]. The inset indicates the area of the main plot. Geological legend: h1: anthropic fill (Holocene); g2: coastal deposits (Holocene); b2: colluvial detrital deposits; ba and bb: alluvial deposits (Holocene); bn: fluvial terraces deposits (Holocene); gn: marine terraces deposits (Upper Pleistocene); MSS: Gravels and Sands of Messina Fm. (Middle Pleistocene); ORDa: calcarenites of San Corrado Fm. (Middle Pleistocene); PTCa: dark gray clays of San Pier Niceto Fm. (Tortonian); PTCb: sandstones low cemented light gray of San Pier Niceto Fm. (Tortonian); PTCc: conglomerate slow cemented of San Pier Niceto Fm. (Tortonian); PMAa: high-grade metamorphic rocks of Aspromonte unit. Continued and dashed red lines: certain and inferred normal faults, respectively. The bathymetric lines are taken from Chiocci et al. [2021]. The blue and black dotted bathymetric lines are taken from Chiocci et al. [2021] and Baratta [1910], respectively.

For this study we have collected the data available in the INGV bulletin [http://terremoti.ingv.it/, ISIDe Working Group, 2007] for the shallow earthquakes occurred during 2000-2021 in the area of Figs 1b and 2a, representing the main territory of the town of Messina. We have selected the earthquakes recorded at a minimum of 6 stations in a radius of 100 km from the epicenter, for which a minimum of 12 P+S arrival times were available. The final dataset includes earthquakes of magnitude in the range 1-3.8. There is no specific estimate of the completeness magnitude

of the bulletin for our study area and period. Completeness magnitude values of the order of 1.6 were reported for the whole Italian area over the last few decades [Lolli et al., 2020]. We consider that the quite favorable location of our study area with respect to the monitoring network operating in the last two decades (Figure 5a) may imply a slightly lower value of the completeness magnitude of our dataset. In any case, small losses of events basically concentrated near the lower bound of the whole magnitude range 1.0-3.8 of the final dataset, say below 1.3-1.4, can be expected.

We have performed hypocenter locations of earthquakes of this final dataset using (i) the arrival times of P and S waves reported in the INGV bulletin (http://terremoti.ingv.it/, ISIDe Working Group, 2007), (ii) the local seismic velocity structure of Orecchio et al. [2011] and (iii) the Bayloc non-linear probabilistic method of Presti et al. [2004]. Bayloc computes for the individual earthquake a probability density cloud with shape and size related to all factors involved in the location process, including the network geometry around the hypocenter (i.e., the cloud marks the hypocentre location uncertainty). Individual earthquake point-locations are also released by Bayloc, which performs a one-step linearized hypocenter location at the end of the Bayesian process, starting from the grid point

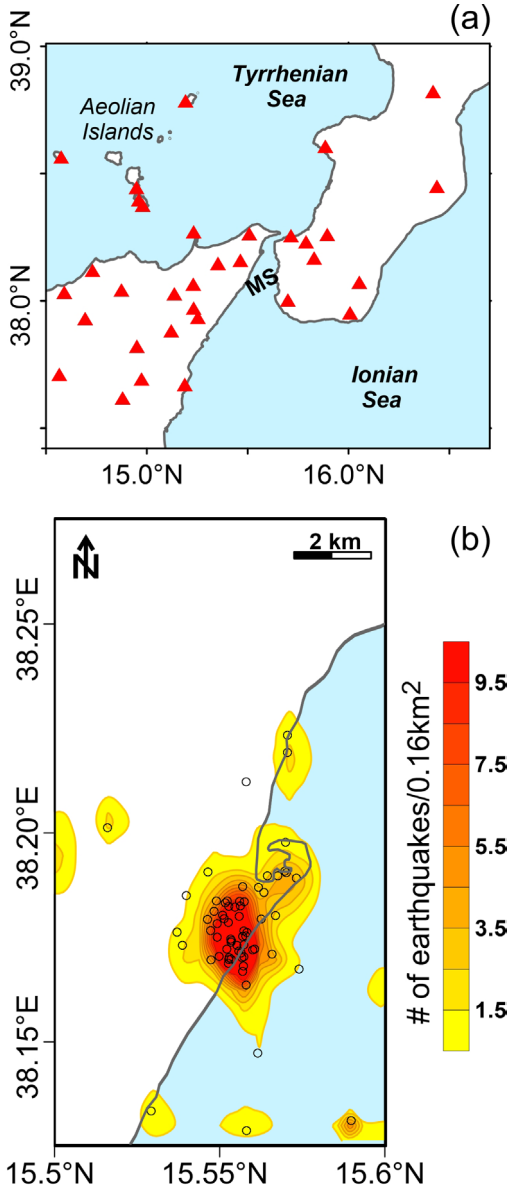

Figure 5. Plot (a) displays the map of seismic stations used for hypocenter locations in the present study. Plot (b) shows the epicentral map obtained by the Bayloc probabilistic location method [Presti et al., 2004] for the earthquakes of magnitude > 1.0 that occurred between January 2000 and December 2021 at depths less than 20 km in the Messina city area. The epicentral distribution is represented both as cumulative probability density and individual earthquake point-locations (see text for details).

of highest probability [see Presti et al., 2004 for details]. The spatial distribution of probability density relative to a set of earthquakes can be computed as the sum of probability density functions of the individual events (joint probability density). Epicentral density maps and hypocentral density sections can be obtained by integration of the joint probability density over horizontal and vertical planes, respectively [a detailed description of the method is given in Presti et al, 2004]. ISOTEST [Presti et al., 2008] is a test using the above concepts and procedures to verify whether a spatial trend of epicenters/hypocenters indicates the geometry of the fault which produced the activity or, alternatively, the observed trend is an artifact of the location process depending, in particular, from poor distribution of seismic stations. ISOTEST is based on (i) isotropic synthetic generation of hypocenters inside the real sequence volume, (ii) positioning around each generated hypocenter of the probability distribution of the real earthquake closest to it, and (iii) statistical comparison of the probability function relative to the sequence under investigation with the probability functions coming from steps (i) and (ii). More precisely, 1000 data sets (d_i) are generated, each of them including a number of synthetic events equal to the number N of earthquakes in the real sequence. By positioning around each synthetic hypocentre the probability distribution of the closest real earthquake, the 1000 probability distributions $D_i(x, y, z)$ relative to the data sets d_i are determined. Then, the average $A(x, y, z)$ of the 1000 probability distributions $D_i(x, y, z)$ is computed. Finally, the misfits M_i between A and each individual distribution D_i, and the misfit M_R between A and the real sequence probability distribution R, can be estimated. In this procedure, A is taken as the reference model of earthquake isotropic generation biased by the location process anisotropy, D_i are random fluctuations around the model, and R is the observed distribution to compare with the model. If M_R lies inside the range of M_i values, we consider that the real sequence hypocentral trend may derive from the combination of the isotropic generation process with anisotropy produced by ill-conditioning of the location process. In this case, the trend can be really suspected of being an artifact of the location process. When M_R is out of the M_i range we argue that the trend cannot be only ascribed to ill-conditioning of the location process and reasonably marks the orientation of the source.

Figures 5 and 6 display the results obtained in the present study by application of Bayloc to the recent seismicity of the Messina area. Figure 5a shows the network of stations used for the analysis. Figure 5b displays the epicentral map in terms of cumulative probability density and point-locations of the individual earthquakes. Figure 6 reports Bayloc's locations obtained for earthquakes occurring in three different periods (23 December 2013, 17 earthquakes; 23-28 December 2013, 28 earthquakes; 2014, 20 earthquakes). For each of these subsets, the figure shows the epicentral map (left) and the hypocentral vertical section perpendicular to the epicentral trend (right). Both point-locations of the individual earthquakes and cumulative probability distributions are reported. Figure 7 shows the result of ISOTEST applied to the three sets of 23 December 2013, 23-28 December 2013 and 2014, respectively. In all cases the misfit M_R is much larger than M_i values and this indicates that the epicentral and hypocentral trends obtained for the respective periods are meaningful, i.e. they are not artifacts of the location process.

3.2 Geology and geomorphology

In the sector of Messina city most affected by seismicity during 2000-2021 (Figure 5) different kinds of geological and geomorphological data are available. The sea-bottom morphology (Figure 8) outlines a 300 m-high bulge facing the city of Messina [Ridente et al., 2014], just where the feature known as *La Falce* is located. The origin of this feature is controversial and has been related to the interplay between the seafloor irregularities and long shore sediment transport [Guarnieri et al., 2004] and/or to the displacement of the crystalline/metamorphic basement by NE-SW and NW-SE normal faults [e.g. Del Ben et al., 1996, 2008]. In particular, NW-SE and NE-SW faults are reported offshore, north and east of *La Falce*, respectively (see Fg and MTF in Figure 8). The presence of a crystalline basement under *La Falce*, between the "Cittadella" and the "Montorsoli lighthouse" (Figures 4 and 8), has been suggested by Cortese [1909], Franchi [1909] and Baratta [1910]. In particular, Cortese [1883; 1888; 1909], and more recently Bonfiglio et al. [1994], propose that the spit which extends east of the Messina harbour (*La Falce*) is built up of metamorphic rocks, Pleistocene conglomerates and overlying incoherent sand deposits.

Guarnieri et al.'s [2004] seismic sections available in the immediate offshore of *La Falce*, corresponding to the seismic profiles SP8 and SP9 indicated in Figure 8, allow to identify the deposition geometry of "Gravels and Sands of Messina Fm" in our study area. In particular, the east-trending seismic section corresponding to SP9 reveals an unconformity interface "B" between this formation and an uncertain substrate (Figure 9). In the same section, the deepest reflector "Z", probably the top of the crystalline units, can be clearly detected only in the centre and in the

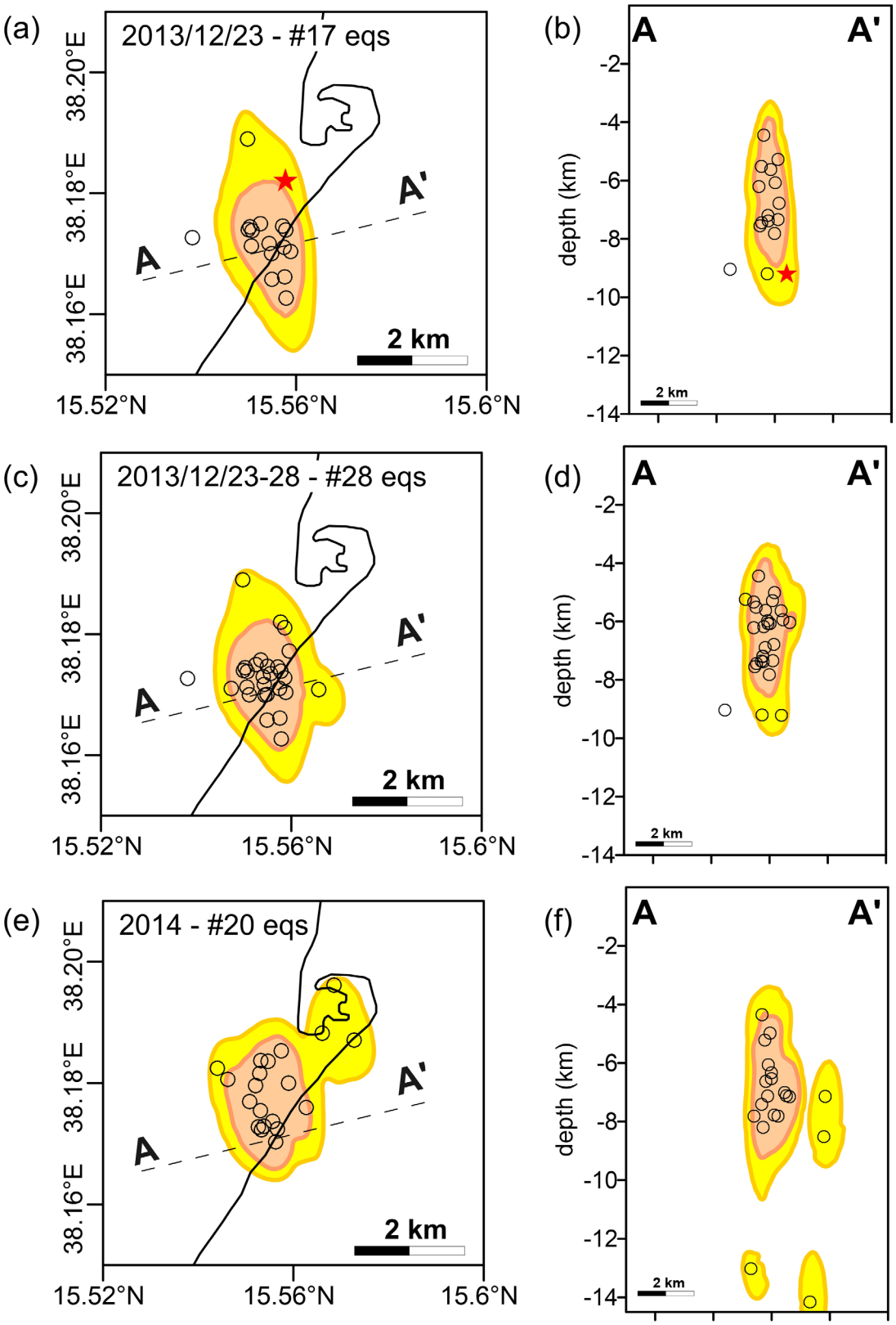

Figure 6. Epicentral maps and vertical sections obtained by Bayloc for subsets of the 2000-2021 earthquakes. In detail: plots (a) and (b) refer to seismicity of the first day of the December 2013 small sequence (23 December 2013); plots (c) and (d) refer to seismicity of the period 23-28 December 2013; plots (e) and (f) refer to seismicity occurred in the same area during 2014. The earthquake spatial distributions are represented both in terms of cumulative probability density (90% and 68% contours are shown) and individual earthquake point-locations. The red star in the plots (a) and (b) indicates the point-location of the first and strongest event of the DEC13 sequence, occurred on 23 December 04:20 GMT (magnitude 3.8).

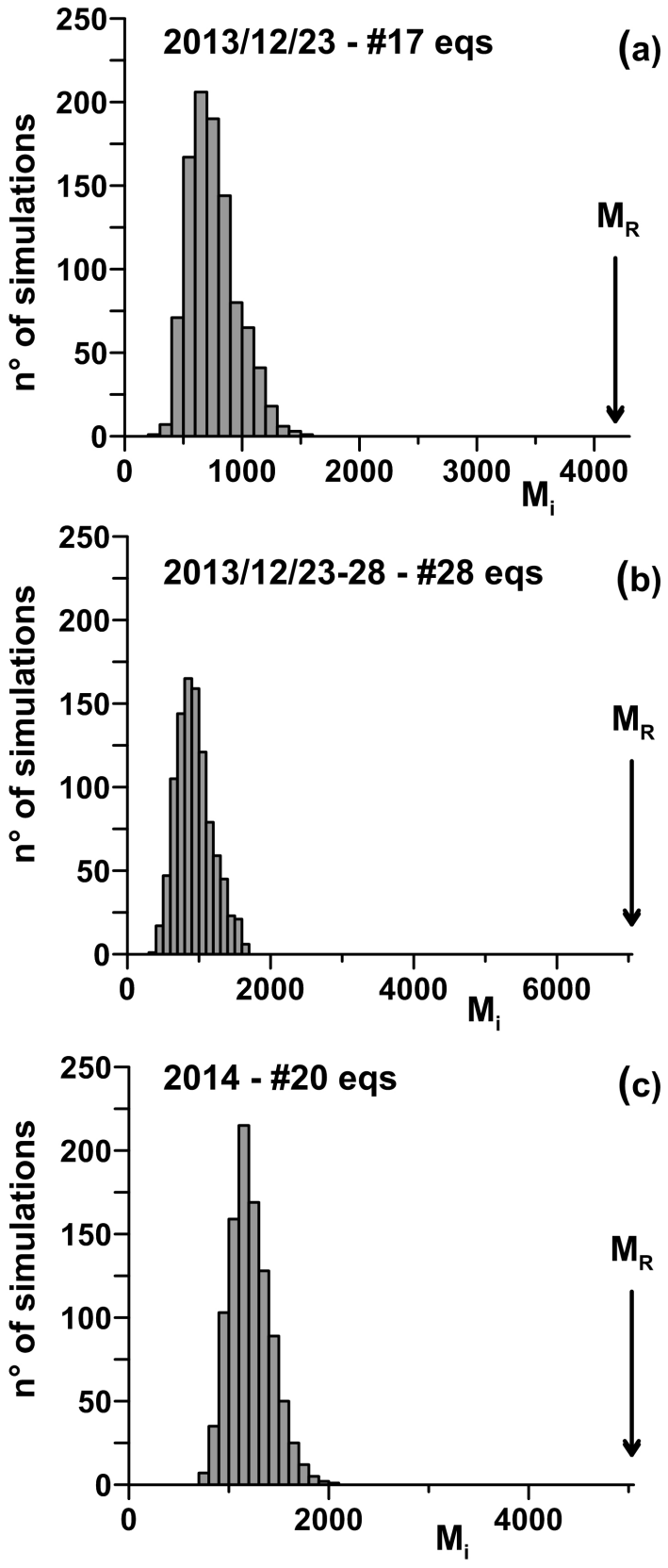

Figure 7. The figure shows the results of the application of ISOTEST procedure [Presti et al., 2008] to the three earthquake subsets of Figure 6, in terms of frequency histograms of the misfits M_i between 1000 random fluctuations of the isotropic model and the model itself (see text for greater detail). The arrow indicates the misfit M_R between the real sequence and the isotropic model. In all cases, the misfit M_R is much larger than M_i values, thus indicating that the epicentral and hypocentral trends obtained for the respective subsets/periods are meaningful, i.e. they are not artifacts of the location process.

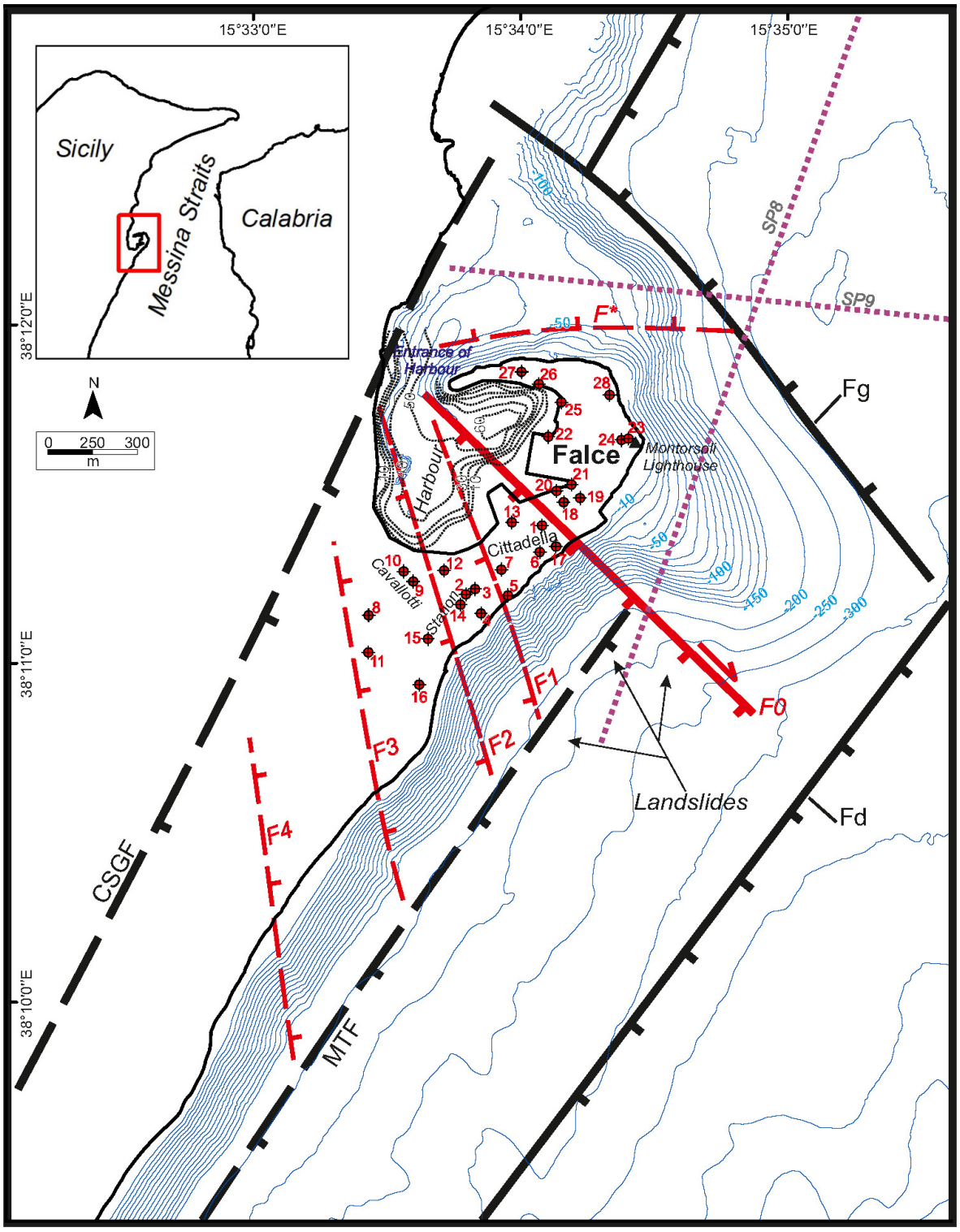

Figure 8. Map of the *La Falce* area with indication of borehole sites and structural features. Red crossed dots with numbering indicate the sites of boreholes kindly furnished for the present study by the Geological Office of Municipality of Messina (public works) and a local professional company (A. Natoli, personal communication). Borehole stratigraphic reconstructions performed in the present study are reported in Figure 10. The faults F0-F4 and F* have been inferred in the present study mainly by analysis of patterns of bathymetric curves, with black and blue bathymetric curves taken from Baratta [1910] and Chiocci et al. [2021], respectively. The fault Fd is taken from Del Ben et al. [1996], Fg is from Guarnieri et al. [2004], CSGF (Capo Scaletta – Grotte fault) is from Selli [1979], MTF (Messina-Taormina fault) is from Dorsey et al. [2023]. Purple dotted lines SP8 and SP9 correspond to parts of seismic profiles 8 and 9 of Guarneri et al. [2004]. Black arrows show landslide areas identified by morpho-bathymetric reconstruction [Ferranti et al., 2008; Ridente et al., 2014; Longhitano, 2018].

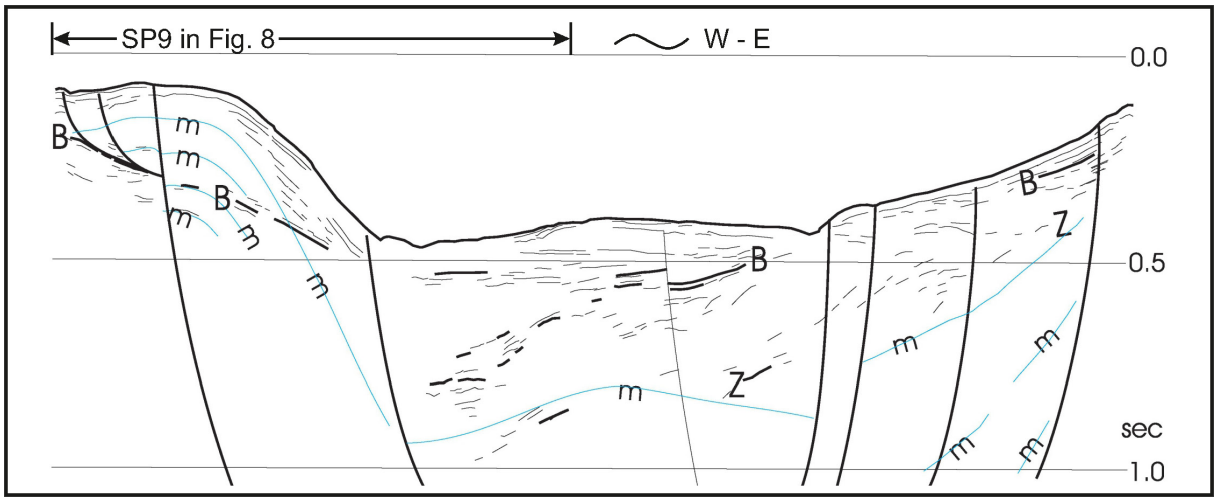

Figure 9. Offshore, ~E-W seismic section 9 of Guarnieri et al. [2004]. The left part of this Section corresponds to our study area (see SP9 in Figure 8). The build-up of *Ghiaie e Sabbie di Messina* in the offshore of Messina city is highlighted and their down-lap deposition is still evident, with an E-sloping unconformity "B" on the base between this formation and an uncertain substrate. In the deeper part of the Section, the W-sloping reflectors from the Calabrian margin (right) suggest a normal fault system on the Sicily shore that originated the extensive tectonics in this region in Pliocene time [Guarnieri et al., 2004]. The following deposition of *Ghiaie e Sabbie di Messina* seems to be particularly concentrated on the footwall of the fault system, whereas in the deep sector and on the Calabria margin it becomes much thinner [Guarnieri et al., 2004]. The deepest reflector "Z" is probably the top of the crystalline units. Strong multiple noise indicated with "m".

Calabrian margin of the Strait, therefore externally to the *La Falce* area. This information does not support inferences of other authors [Cortese, 1909; Franchi, 1909; Baratta, 1910; Bonfiglio et al., 1994] concerning the presence of crystalline units at shallow depth beneath *La Falce*.

A wide set of borehole data has been collected in the present study from the Geological Office of Municipality of Messina (public works) and a local professional company (A. Natoli, personal communication). The data collected for *La Falce* area and the coastal plain of Messina city are shown in Figure 10, with the site locations indicated in Figure 8. The data of Figure 10 (maximum exploration depths of 43 meters in the *La Falce* area and 60 meters in the city coastal plain) reveal the presence of coarse grained loose "Gravels and Sands of Messina Fm.", underlying up to 8m thick alluvial and coastal deposits occasionally featuring well-cemented metric levels of conglomerates. The data never show the presence of crystalline unit in the explored depth ranges. The same data, which are mainly distributed along a NE-SW direction (see map of Figure 8), do not allow to identify stratigraphic interfaces or marker lithological layers useful for evaluation of spatial heterogeneities and/or vertical displacements of stratigraphic successions.

A striking feature of morphobathymetric curves can be noted in the eastern offshore of *La Falce* [Figure 8; Guarnieri et al., 2004; Ridente et al., 2014; Chiocci et al., 2021]. Here, the NE-trending steep slope curves following the coastline south of *La Falce* show an abrupt change of direction of about 90° towards SE, delineating the southern border of the already mentioned bulge (see Figures 4 and 8). The same feature marks the transition between the southern offshore sector of *La Falce*, characterized by widespread sea-bottom morphological irregularities, and the northern one where the bathymetry is more regular and uniform (Figure 8). Seafloor irregularities in the southern sector have been related to coalescing multiple large landslide scars very close to the shoreline (Figure 8; Ferranti et al., 2008; Ridente et al., 2014; Longhitano, 2018; Chiocci et al., 2021]. In particular, down-slope of the scars, seismic profiles suggest the existence of a rotational slide rooted at ~0.7 s TWT which involves the entire Quaternary seismostratigraphic unit [Ferranti et al., 2008]. The occurrence of large landslides is often controlled by tectonic, topographical and lithological features [e.g. Van Westen et al., 2008; Glade et al., 2005; Conforti and Ietto, 2020]. Considering that the two (southern and northern) sectors display similar seafloor slope angle conditions [Chiocci et al., 2021], the slope instability in the southern one can more likely be related to lithological/geotechnical and/or tectonics factors.

The striking pattern of bathymetric curves at the southern border of the bulge leads us to hypothesize the presence of a NW-SE trending normal fault with dextral strike-slip component that we indicate as F0 in Figure 8. Clear

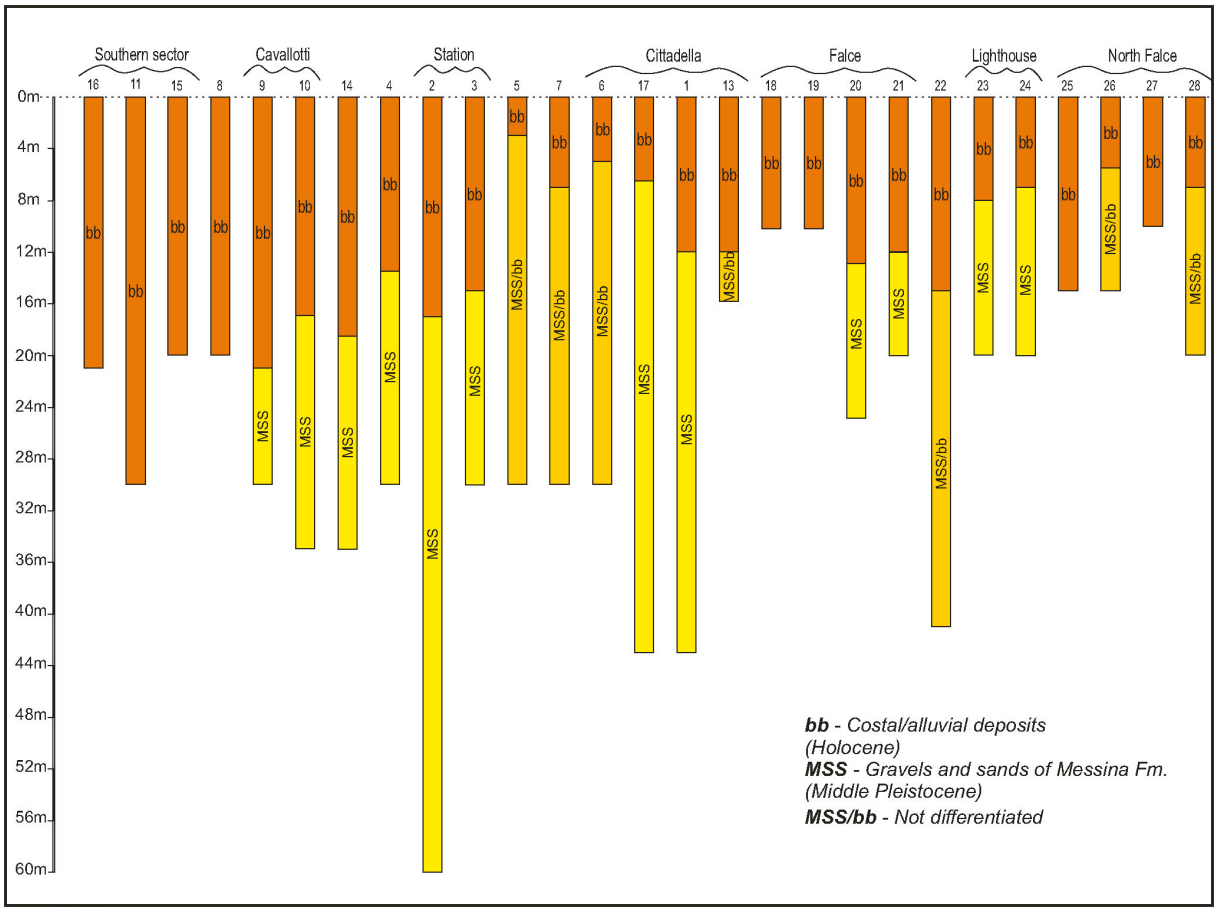

Figure 10. Stratigraphic reconstructions obtained from borehole data kindly furnished for the present study by the Geological Office of Municipality of Messina (Territorial Data archive) and a local professional company (A. Natoli, personal communication). Borehole sites are indicated in the map of Figure 8.

irregularities in the bathymetric lines along the coastal slope south of the bulge are coherent with the presence of a bundle of NNW-SSE normal faults that we tentatively trace as red dashed lines (F1 to F4) in Figure 8. It can also be noted in Figure 8 that the potential faults F1 and F2 seem also to be constrained in the harbor area by the bathymetric curves reported in Baratta [1910] and Chiocci et al. [2021], respectively. The structural scenario defined by faults F0 to F4 (Figure 8), closely matching with the sector where most of recent seismicity has been located (Figure 5), would mark internal deformation of the local horst documented by previous authors [e.g, Ghisetti, 1984; Guarnieri et al., 2004] roughly in the same area. We propose this analysis of morphobathymetric data and concerned mechanisms on the seafloor of the Strait as a preliminary approach to exploration of faults and tectonic features in the offshore part of our study area, in analogy with what has been already done by previous investigators [see, e.g., Ridente et al., 2014]. Detecting signatures of possible faults may pave the way for new investigations and this may be a significant contribution in a sector where the structural information on a local scale is poor and/or the local geology is complex. As regard to our analysis, it can be worth mentioning that an independent, concomitant investigation has led Dorsey et al. [2023] to suggest the presence of a NW-SE trending fault in close correspondence with our fault F0.

4. Discussion and conclusion

The greatest part of the recent, shallow seismicity of the Messina area occurred in the part of the town including the *La Falce* geological structure and the coastal zone immediately southwest of it (Figure 5). Southwest of *La Falce*, the Bayloc point-locations and cumulative probability distribution highlight a clear epicentral trend oriented NNW-SSE. Minor additional activity without a really detectable trend can be noted just in correspondence with *La Falce*. Focusing on the seismicity which occurred more concentrated in time (the small sequence of December 2013

and the subsequent activity of 2014) we attempt to obtain greater accuracy in the detection of the fault (or the faults) which may have played a role in the generation of the seismicity in argument. The panels 'a' and 'b' of Figure 6 (the first part of the sequence corresponding to 17 earthquakes) show that the events occurred in the depth range 4-9 km approximately, on a NNW-trending, subvertical plane. Quite similar information can be obtained from the analysis of all 28 earthquakes of the sequence (23-28 December 2013; panels 'c' and 'd' of Figure 6), even if in this case a slightly greater dispersion of the events can be noted. The panels 'e' and 'f' of Figure 6 (seismicity of 2014) evidence greater dispersion of the events, with the permanence, however, of most activity in the area of the seismolineament of the 2013 sequence. As said in a previous paragraph, the ISOTEST (Figure 7) proves that the epicentral and hypocentral trends obtained for the respective periods are meaningful, i.e. they are not artifacts of the location process, therefore they can be used for structural interpretation of seismicity.

Figure 11 reports the epicentral map (a) and the hypocenter vertical section (b) relative to the first phase of the sequence, together with the focal mechanism of the first and strongest event taken from Neri et al. [2021]. This focal mechanism was computed by the waveform inversion method known as CAP [Zhao and Helmberger, 1994; Zhu and Helmberger, 1996; D'Amico et al., 2010 and 2011] which is able to furnish well constrained solutions also for earthquakes of magnitude below 4, diversely from other, widely used waveform inversion methods [Dziewonski et al., 1981; Pondrelli et al., 2006; Ekstrom et al., 2012]. On their hand, Pino et al. [2023] used the Gillard et al. [1996] criterion to compare the nodal planes of this mechanism with the local stress tensor and found that the nodal plane which may have acted as the fault plane is the NNW-striking WSW-dipping one. The waveforms available for the other earthquakes of the small sequence, all of magnitude less than 3, have not permitted the computation of stable focal mechanisms.

The map of Figure 11a displays also the faults reported in the literature for the specific sector under investigation and some additional faults suggested in the Section 3b of the present study on the basis of geological and morphobathymetric data. The latter are also tentatively traced in the vertical section of the Figure 11b. The data available for the seismic sequence of 23 December 2013 can be associated to the structural pattern inferred for the same area. In particular, the sequence (showing a clear NNW-SSE epicentral trend) is located in the sector of the structures indicated as F0-F4, striking between NW-SE (F0) and NNW-SSE (F1 to F4), and diversely dipping (east-ward the western ones F4 and F3, and west-ward the eastern ones F2 to F0). The location and focal mechanism of the first, strongest and deepest event of the sequence (with the 67°, SW-dipping nodal plane identified as the fault plane) lead us to guess that this event may have occurred at ca. 9 km depth on fault F0. Based on hypocentral locations defining an almost vertical east-dipping seismolineament in the cross-section of Figure 11b, the other events of the small sequence could be associated to fault F4. The latter events, located in the depth range 4-9 km, could plausibly have been induced by stress perturbation due to the first, deeper and stronger event, according to a process typical of areas with horst/graben dynamics [e.g. Davis and Reynolds, 1996]. The Messina Strait area is affected by horst/graben dynamics, with the Peloritani and Aspromonte mountain chains working as main horsts and the Strait as main graben. As already said in the previous Sections, minor horsts have been identified in the overall basin area, one of which approximately located in the area of *La Falce* and surroundings [e.g. Ghisetti, 1984; Guarnieri et al., 2004]. The NW-trending fault reported by Guarnieri et al. [2004] *ca.* 1 km north of *La Falce* (Fg in the Figures 8 and 11a), together with the fault F* we have traced in the same Figures 8 and 11a on the basis of morphobathymetric curves taken from Chiocci et al. [2021], may be identified as the step-like northern border of the *La Falce* horst. Unfortunately, the information and data today available do not allow detection of the southern boundary of the horst. We may concur to current studies of structures and their dynamic relationships in this very complex area by suggesting that the small sequence of December 2013 (and most of seismicity recorded in the Messina area during 2000-2021) may reflect minor horst/graben dynamics on the Sicilian coast of the Strait, in correspondence with the historical center of Messina. In other words, the present study attempts to frame the local-scale features detected over the Messina area in the tectonic scenario of Messina Strait furnished by previous investigators [Ghisetti, 1984 and 1992; Del Ben et al., 1996 and 2008; Guarnieri et al., 2004].

Finally, the Figure 11a allows us to observe also the location of recent seismicity and geological features compared to the location of the upper edge of the 1908 earthquake source as reported in the INGV DISS Database [DISS Working Group, 2021]. As said above (see also Figure 1a for a whole graphical representation of the source), the upper edge of this source is positioned at 3 km depth. With an interesting laboratory experiment, Bonini et al. [2011] showed that 1908-like earthquakes occurring on a blind fault similar to that indicated in the DISS database may produce surficial or very shallow dislocations and faults with orientations broadly parallel to the main source. A deep investigation of the nature of the NNE-trending faults documented on land and offshore in the Messina area near the upper edge of the DISS 1908 source is out of the purposes of the present study. However, we cannot avoid

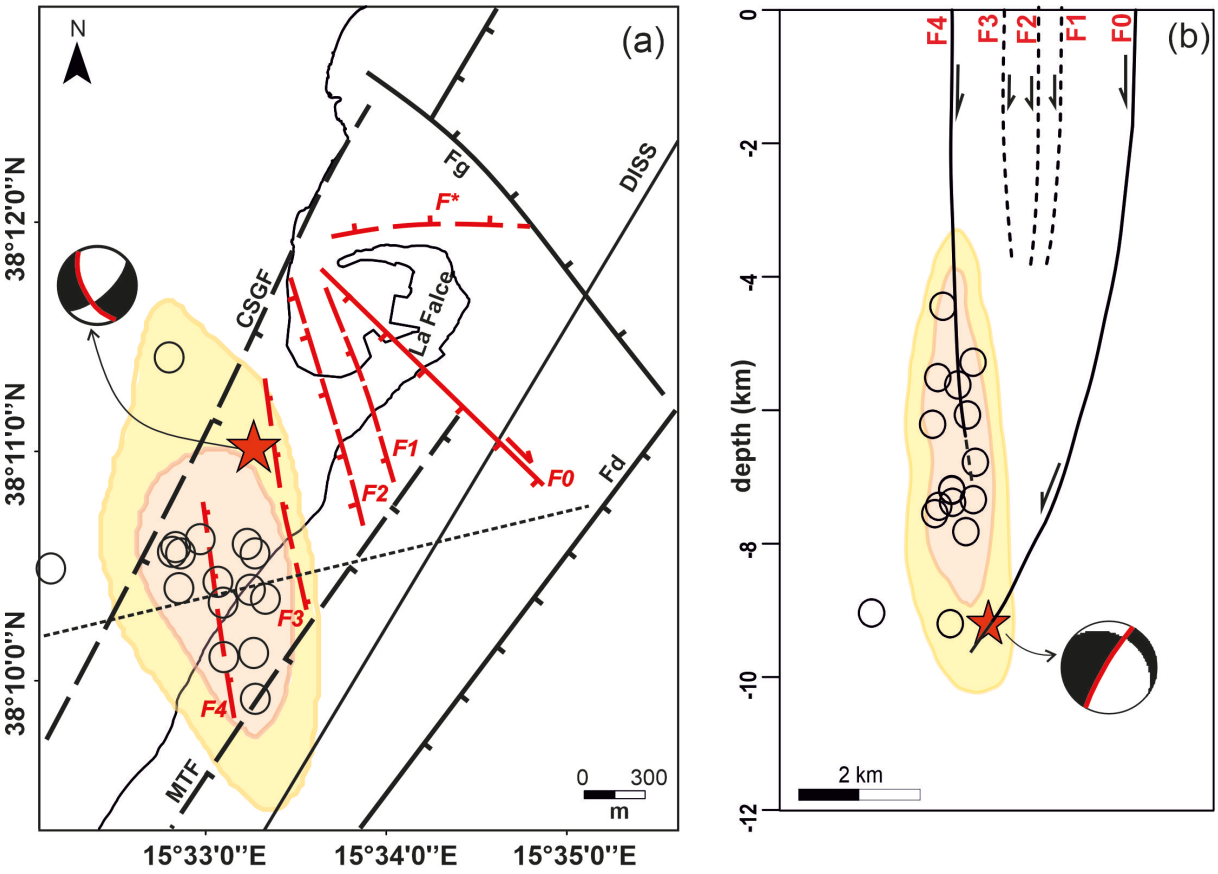

Figure 11. Summary of the main findings of the present work. The map in plot (a) displays the faults reported in the literature for the specific sector under investigation (black lines) and some additional faults inferred in present study from geological and morphobathymetric data (red lines). The latter are also tentatively traced in the vertical section of plot (b), the profile of which is represented by the dotted segment in the map. The figure also reports the epicentral map (a) and hypocentral vertical section (b) relative to the first phase of the December 2013 small sequence, together with the focal mechanism of the first and strongest event of the sequence taken from Neri et al. [2021]. As in the case of Figure 6, the earthquake spatial distributions are represented both in terms of cumulative probability density (90% and 68% contours) and individual earthquake point-locations. The red star in the plots (a) and (b) indicates the point-location of the first and strongest event of the DEC13 sequence, occurred on 23 December 04:20 GMT (magnitude 3.8). The seismicity and the structural pattern of F0 to F4 faults show a pretty good correspondence that we explain in terms of dynamics of minor horst/graben structures on the Sicilian coast of the Strait.

noting that the Messina-Taormina fault, widely documented in the literature [e.g., Selli, 1979; Pavano et al., 2016; Meschis et al., 2019] and traced in our Figures 8 and 11 according to the most recent study of Dorsey et al. [2023], stops just in correspondence with the southern border of the *La Falce* bulge [Figures 8 and 11]. This structural pattern leads to suspect a role of the bulge and related geological features in conditioning faults reputed of some relevance (such as the Messina-Taormina fault), eventually in connection with the activity of the DISS 1908 blind fault. The sector of Messina territory which was seismically most active during 2000-2021 is very close to the DISS 1908 source and possible relationships could exist between the same sector and the shallow effects of the blind, main source. Future further deepening of investigations in this area seems appropriate to us.

Acknowledgements. We thank the Editor and two anonymous reviewers for constructive comments that have allowed us to improve the paper. We are also grateful to Dr. Alfredo Natoli (Geotre s.a.s. Messina) and to Messina Municipality for furnishing borehole data used in the present study. This research has benefited from funding provided by PO-FESR 2014/2020, ID 08CT2790090212 Project 'HCH LowCostGeoEngineering Check'.

References

Amato, A. and F. Mele (2008). Performance of the INGV National Seismic Network from 1997 to 2007, Ann. Geophys., 51, 2-3, doi:10.4401/ag-4454

Argnani, A. (2022). Comment on the paper by Barreca et al.: "The Strait of Messina: Seismotectonics and the source of the 1908 earthquake", Earth-Sci. Rev., 226, 103961, doi:10.1016/j.earscirev.2022.103961

Argnani, A. and N.A. Pino (2023). The 1908 Messina Straits Earthquake: Cornerstones and the Need to Step Forward, Seismol. Res. Lett., 94, 2A, 557-561.

Baratta, M. (1910). La catastrofe sismica Calabro messinese (28 dicembre 1908), Presso la Società geografica italiana.

Barreca, G., F. Gross, L. Scarfì, M. Aloisi, C. Monaco and S. Krastel (2021). The Strait of Messina: Seismotectonics and the Source of the 1908 Earthquake, Earth-Sci. Rev., 218, 103685, doi:10.1016/j.earscirev.2021.103685

Billi, A., D. Presti, B. Orecchio, C. Faccenna and G. Neri (2010). Incipient extension along the active convergent margin of Nubia in Sicily, Italy: Cefalù-Etna seismic zone, Tectonics, 29, 4.

Bonfiglio, L., G. Bacci, D. Barra, I. Di Geronimo, G. Bonaduce, L. Manfra, A. Proposito and D. Violanti (1994). Paleoecological, radiometric and archeological core analysis of Holocene deposits in the Messina harbour area (North-Eastern Sicily), Bollettino della Società Paleontologica Italiana, 47-60.

Bonini, L., D. Di Bucci, G. Toscani, S. Seno and G. Valensise (2011). Reconciling Deep Seismogenic and Shallow Active Faults through Analogue Modelling: the Case of the Messina Straits (Southern Italy), J. Geol. Soc. 168, 1, 191-199. doi:10.1144/0016-76492010-055

Bottari, A., P. Capuano, G. De Natale, P. Gasparini, G. Neri, F. Pingue and R. Scarpa (1989). Source parameters of earthquakes in the Strait of Messina, Italy, during this century, Tectonophysics, 166, 1-3, 221-234.

Chiocci, F.L., F. Budillon, S. Ceramicola, F. Gamberi and P. Orrù (2021). Atlante Dei Lineamenti Di Pericolosità Geologica Dei Mari Italiani Risultati Del Progetto Magic; CNR Edizioni: Roma, Italy; ISBN 978-88-8080-457-4

Conforti, M. and F. Ietto (2020). Influence of tectonics and morphometric features on the landslide distribution: a case study from the Mesima Basin (Calabria, South Italy), J. Earth Sci., 31, 2, 393-409.

Cortese E. (1883). Sulla formazione dello Stretto di Messina, Boll. R. Comitato, Geol. It., 13: 4-39.

Cortese E. (1888). Sulla origine del porto di Messina e sui movimenti di mare nello Stretto, Boll. Soc. Geol. It., 7, 416-422.

Cortese E. (1909). Una sezione geologica attraverso il Peloro, lo Stretto di Messina e l'Aspromonte, Boll. Soc. Geol. It., 28, 3, c445-468.

D'Amico, S., B. Orecchio, D. Presti, A. Gervasi, L. Zhu, I. Guerra, G. Neri, and R.B. Herrmann (2011). Testing the Stability of Moment Tensor Solutions for Small Earthquakes in the Calabro-Peloritan Arc Region (Southern Italy), Boll. Geof. Teor. Appl. 52, 283-298., doi:10.4430/bgta0009

D'Amico, S., B. Orecchio, D. Presti, L. Zhu, R. B. Herrmann and G. Neri (2010). Broadband Waveform Inversion of Moderate Earthquakes in the Messina Straits, Southern Italy, Phys. Earth Planet. In. 179, 97-106. doi:10.1016/j.pepi.2010.01.012

Davis H.G. and S.J. Reynolds (1996). Structural Geology, Wiley & Son Inc. New York, 776.

Del Ben, A., C. Gargano and R. Lentini (1996). Ricostruzione strutturale e stratigrafica dell'area dello Stretto di Messina mediante analisi comparata dei dati geologici e sismici, Mem. Soc. Geol. It., 51, 703-717.

Del Ben, A., C. Barnaba and A. Taboga (2008). Strike-slip systems as the main tectonic features in the Plio-Quaternary kinematics of the Calabrian Arc, Marine Geophys. Res., 29, 1-12.

Dewey, J. F., M. L. Helman, S.D. Knott, E. Turco and D. H. W. Hutton (1989). Kinematics of the western Mediterranean, Geological Society, London, Special Publications, 45, 265-283 https://doi.org/10.1144/GSL.SP.1989.045.01.15

DISS Working Group (2021). Database of Individual Seismogenic Sources (DISS), Version 3.3.0: A compilation of potential sources for earthquakes larger than M 5.5 in Italy and surrounding areas. Istituto Nazionale di Geofisica e Vulcanologia (INGV), https://doi.org/10.13127/diss3.3.0

Doglioni, C., M. Ligi, D. Scrocca, S. Bigi, G. Bortoluzzi, E. Carminati, M. Cuffaro, F. D'Oriano, V. Forleo, F. Muccini and F. Riguzzi (2012). The tectonic puzzle of the Messina area (Southern Italy): Insights from new seismic reflection data, Scientific Reports, 2, 1, 1-9.

Dorsey, R., S. Longhitano and D. Chiarella (2023). Structure and Morphology of an Active Conjugate Relay Zone, Messina Strait, Southern Italy, Basin res, https://doi.org/10.31223/X5PH2J, in press.

Dziewonski, A. M., T.-A. Chou and J. H. Woodhouse (1981). Determination of earthquake source parameters from waveform data for studies of global and regional seismicity, J. Geophys. Res., 86, 2825-2852, doi:10.1029/JB086iB04p02825

Ekström, G., Nettles, M., and A. M. Dziewonski (2012). The Global CMT Project 2004-2010: Centroid-Moment Tensors for 13,017 Earthquakes, Phys. Earth Planet. In., 200, 1-9, doi:10.1016/j.pepi.2012.04.002

Faccenna, C., P. Molin, B. Orecchio, V. Olivetti, O. Bellier, F. Funiciello, L Minelli, C. Piromallo and A. Billi (2011). Topography of the Calabria subduction zone (southern Italy): Clues for the origin of Mt. Etna, Tectonics, 30, 1.

Ferranti, L., C. Monaco, D. Morelli, R. Tonielli, L. Tortorici and M. Badalini (2008). Morphostructural setting and active faults in the Messina Strait: new evidence from marine geological data, Rendiconti Online della Società Geologica Italiana, 1, 86-88.

Finetti, I. and A. Del Ben (1986). Geophysical Study of the Tyrrhenian Opening, Boll. Geof. Teor. App., 28, 75-155.

Finetti, I.R., F. Lentini, S. Carbone, S. Catalano and A. Del Ben (1996). Il sistema appenninico meridionale-arco calabro-Sicilia: studio geologico-geofisico, Boll. Soc. Geol. It., 115, 529-559.

Franchi, S. (1909). Il terremoto del 28 dicembre 1908 a Messina, in rapporto alla natura del terreno ed alla riedificazione della città, Boll. Comit. Geol. Ital, 111-157.

Gargano, C. (1994). Carta geologica di Messina e del settore nord-orientale dei Monti Peloritani, Università di Catania, Istituto di Geologia e Geofisica, scala 1:25.000. S.EL.CA., Firenze

Ghisetti, F. (1981). L'evoluzione strutturale del bacino plio-pleistocenico di Reggio Calabria nel quadro geodinamico dell'Arco Calabro, Boll. Soc. Geol. It., 100, 433-466.

Ghisetti, F. (1984). Recent deformations and the seismogenic source in the Messina Strait (southern Italy), Tectonophysics, 109, 191-208, doi:10.1016/0040-1951(84)90140-9

Ghisetti, F. (1992). Fault Parameters in the Messina Strait (Southern Italy) and Relations with the Seismogenic Source, Tectonophysics, 210, 1-2, 117-133, doi:10.1016/0040-1951(92)90131-o

Ghisetti, F. and L. Vezzani (1982). Different styles of deformation in the Calabrian arc (southern Italy): implications for a seismotectonic zoning, Tectonophysics, 85, 3-4, 149-165, https://doi.org/10.1016/0040-1951 (82)90101-9

Gillard, D., M. Wyss and P. Okubo (1996). Type of faulting and orientation of stress and strain as a function of space and time in Kilauea's south flank, Hawaii J. Geophys. Res., 101, 16025-16042, Doi: 10.1029/96JB00651

Glade, T., M. G. Anderson and M. J. Crozier (2005). Landslide hazard and risk, 807, Chichester, Wiley.

Görgün, E. and A. M. Albora (2017). Seismotectonic investigation of Biga peninsula in SW Marmara region using steerable filter technique, potential field data and recent seismicity, Pure Appl. Geophys., 174, 10, 3889-3904.

Görgün, E., D. Kalafat and K. Kekovalı (2020). Source Mechanisms and stress field of the 2017 Ayvacık/Çanakkale earthquake sequence in NW Turkey, Ann. Geophys. https://doi.org/10.4401/ag-8194

Guarnieri, P., A. Di Stefano, S. Carbone, F. Lentini and A. Del Ben (2004). A multidisciplinary approach to the reconstruction of the Quaternary evolution of the Messina Strait (with Geological Map of the Messina Strait 1:25.000 scale), in Mapping Geology in Italy Pasquarè, G., Venturini, C. (Editor), APAT, Roma, 45-50.

Guarnieri, P. and C. Pirrotta (2008). The response of drainage basins to the late Quaternary tectonics in the Sicilian side of the Messina Strait (NE Sicily), Geomorphology, 95, 3-4, 260-273, doi:10.1016/j.geomorph.2007.06.013

Guidoboni E., G. Ferrari, D., Mariotti, A. Comastri, G. Tarabusi, G. Sgattoni and G. Valensise (2018). CFTI5Med, Catalogo dei Forti Terremoti in Italia (461 a.C.-1997) e nell'area Mediterranea (760 a.C.-1500). Istituto Nazionale di Geofisica e Vulcanologia (INGV), doi: https://doi.org/10.6092/ingv.it-cfti5

Guidoboni, E., G. Ferrari, G. Tarabusi, G. Sgattoni, A. Comastri, Mariotti, C. Ciuccarelli, M. G. Bianchi and G. Valensise (2019). CFTI5Med, the new release of the catalogue of strong earthquakes in Italy and in the Mediterranean area, Scientific Data, 6, 1, 80, doi: 10.1038/s41597-019-0091-9

ISIDe Working Group (2007). Italian Seismological Instrumental and Parametric Database (ISIDe). Istituto Nazionale di Geofisica e Vulcanologia (INGV), https://doi.org/10.13127/ISIDE

Lentini, F. (1999). Carta geologica della Provincia di Messina, scala 1:50.000, 3 fogli. S.EL.CA. (Ed.), Firenze.

Lentini, F., S. Carbone and S. Catalano (1994). Main structural domains of the central mediterranean region and their tectonic evolution, Boll. Geofis. Teor. Appl., 36, 141-144, 103-125.

Lentini, F., S. Carbone, S. Catalano, M. Gargano, M. Romeo, S. Strazzulla and G. Vinci (1995). Sedimentary evolution of basins in mobile belts: examples from the Tertiary terrigenous sequences of the Peloritani Mountains (NE Sicily), Terra Nova, 7, 161-170, https://doi.org/10.1111/j.1365-3121.1995.tb00685.x

Lentini, F., S. Catalano and S. Carbone (2000). Note Illustrative della Carta Geologica della Provincia di Messina, scala 1:50.000. S.EL.CA. (Ed.), Firenze.

Lolli, B., D. Randazzo, G. Vannucci and P. Gasperini (2020). The HOmogenized instRUmental Seismic catalog (HORUS) of Italy from 1960 to present, Seismol. Res. Lett., 91, 6, 3208-3222.

Longhitano, S. G. (2018). Between Scylla and Charybdis (part 2): The sedimentary dynamics of the ancient, Early Pleistocene Messina Strait (central Mediterranean) based on its modern analogue, Earth-Sci. Rev., 179, 248-286, doi:10.1016/j.earscirev.2018.01.017.

Meschis, M., G. P. Roberts, Z. K. Mildon, J. Robertson, A. M. Michetti, and J. P. Faure Walker (2019). Slip on a mapped normal fault for the28th December 1908 Messina earthquake (Mw 7.1), Scientific Reports, 9, 1, 6481, doi: 10.1038/s41598-019-42915-2.

Monaco, C., G. Barreca and A. Di Stefano (2017). Quaternary marine terraces and fault activity in the northern mainland sectors of the Messina Strait (southern Italy), Italian J. Geosci., 136, 3, 337-346, Doi:10.3301/IJG.2016.10

Michelini, A., L. Margheriti, M. Cattaneo, G. Cecere, G. D'Anna, A. Delladio, M. Moretti, S. Pintore, A. Amato, A. Basili, A. Bono, P. Casale, P. Danecek, M. Demartin, L. Faenza, V. Lauciani, A.G. Mandiello, A. Marchetti, C. Marcocci, S. Mazza, F. M. Mele, A. Nardi, C. Nostro, M. Pignone, M. Quintiliani, S. Rao, L. Scognamiglio and G. Selvaggi. (2016). The Italian National Seismic Network and the earthquake and tsunami monitoring and surveillance systems, Adv. Geosci., 43, 31-38.

Monaco, C., and L. Tortorici (2000). Active Faulting in the Calabrian Arc and Eastern Sicily, J. Geodyn., 29 (3-5), 407-424. doi:10.1016/S0264-3707(99)00052-6

Neri, G., G. Barberi, G. Oliva and B. Orecchio (2004). Tectonic stress and seismogenic faulting in the area of the 1908 Messina earthquake, south Italy, Geophys. Res. Lett., 31, 10, doi: 10.1029/2004GL019742

Neri, G., G. Oliva, B. Orecchio and D. Presti (2006). A possible seismic gap within a highly seismogenic belt crossing Calabria and eastern Sicily, Italy, Bull. Seismol. Soc. Am., 96, 1321-1331, doi:10.1785/0120050170

Neri, G., B. Orecchio, S. Scolaro and C. Totaro (2020). Major earthquakes of southern Calabria, Italy, into the regional geodynamic context, Frontiers Earth Sci., 8, 579846.

Neri, G., B. Orecchio, D. Presti, S. Scolaro and C. Totaro (2021). Recent seismicity in the area of the major, 1908 Messina Straits earthquake, south Italy, Frontiers Earth Sci., 9, 667501, doi:10.3389/feart.2021.667501

Orecchio, B., D. Presti, C. Totaro, I. Guerra and G. Neri (2011). Imaging the velocity structure of the Calabrian Arc region (south Italy) through the integration of different seismological data, Boll. Geofis. Teor. Appl. 52, 625-638, doi:10.4430/bgta0023

Pavano, F., F. J. Pazzaglia and S. Catalano (2016). Knickpoints as geomorphic markers of active tectonics: A case study from northeastern Sicily (southern Italy), Lithosphere, 8, 6, 633-648.

Pino, N. A., M. Palano and G. Ventura (2021). Comment on the paper by Barreca et al.: "The Strait of Messina: Seismotectonics and the source of the 1908 earthquake" (Earth-Science Reviews 218, 2021, 103685), Earth-Sci. Rev., 223, 103865, doi: 10.1016/j.earscirev.2021.103865

Pino P., S. Scolaro, A. Torre, S. D'Amico, G. Neri and D. Presti (2023). Geophysical and geological signatures of an unknown fault in the historic center of Messina (Sicily, south Italy), 66, 2023, doi:10.4401/ag-8950.

Pondrelli, S., S. Salimbeni, G. Ekström, A. Morelli, P. Gasperini and G. Vannucci (2006). The Italian CMT Dataset from 1977 to the Present, Phys. Earth Planet. Interiors 159, 3-4, 286-303, doi:10.1016/j.pepi.2006.07.008

Presti, D., B. Orecchio, G. Falcone and G. Neri (2008). Linear versus non-linear earthquake location and seismogenic fault detection in the southern Tyrrhenian Sea, Italy, Geophys. J. Int. 172, 607-618, doi:10.1111/j.1365-246x.2007.03642.x

Presti, D., C. Troise and G. De Natale (2004). Probabilistic location of seismic sequences in heterogeneous media, Bull. Seismol. Soc. Am., 94, 2239-2253, doi:10.1785/0120030160

Ridente, D., E. Martorelli, A. Bosman and F. L. Chiocci (2014). High-resolution morpho-bathymetric imaging of the Messina Strait (Southern Italy). New insights on the 1908 earthquake and tsunami, Geomorphol., 208, 149-159, https://doi.org/10.1016/j.margeo.2013.10.009

Scarfì, L., G. Barberi, C. Musumeci and D. Patanè (2016). Seismotectonics of northeastern Sicily and southern Calabria (Italy): New constraints on the tectonic structures featuring in a crucial sector for the Central Mediterranean geodynamics, Tectonics, 35, 812-832, doi:10.1002/2015TC004022

Schorlemmer, D., F. Mele and W. Marzocchi (2010). A Completeness Analysis of the National Seismic Network of Italy, J. Geophys. Res., 115, B4, doi:10.1029/2008JB006097

Selli, R., P. Colantoni, A. Fabri, S. Rossi, A. M. Borsetti and P. Gallignani (1978). Marine Geological Investigations on the Messina Strait and its approaches, Giornale di Geologia, 42, 2.

Selli, R. (1979). Geologia e sismotettonica dello Stretto di Messina. Convegno su: L'attraversamento dello Stretto di Messina e la sua fattibilità, 4-6 Luglio 1978, Atti Acc. Naz. Lincei, 43, 119-154.

Serpelloni, E., R. Bürgmann, M. Anzidei, P. Baldi, B. M. Ventura and E. Boschi (2010). Strain accumulation across the Messina Straits and kinematics of Sicily and Calabria from GPS data and dislocation modeling, Earth and Planet. Sci. Lett., 298, 3-4, 347-360, doi: 10.1016/j.epsl.2010.08.005

Servizio Geologico di Italia (2008). Carta Geologica d'Italia in scala 1:50.000 – Foglio 601 Messina – Reggio Calabria. Coordinatore F. Lentini. APAT/Regione Siciliana/D.S.G.-Università di Catania. ISPRA.

Van Westen, C. J., E. Castellanos and S. L. Kuriakose (2008). Spatial data for landslide susceptibility, hazard, and vulnerability assessment: An overview, Engin. Geol., 102, 3-4, 112-131.

Zhao, L. S., and D. V. Helmberger (1994). Source Estimation from Broadband Regional Seismograms, Bull. Seismol. Soc. Am. 84, 1, 91-104.

Zhu, L., and D. Helmberger (1996). Advancement in Source Estimation Technique Using Broadband Regional Seismograms, Bull. Seismol. Soc. Am. 86, 1634-1641.

Westaway, R. (1993). Quaternary uplift of southern Italy, J. Geophys. Res.: Solid Earth, 98, B12, 21741-21772. https://doi.org/10.1029/93JB01566

***CORRESPONDING AUTHOR: Giancarlo NERI**,
Department of Mathematics, Computer Sciences, Physics, and Earth Sciences, University of Messina
e-mail: geoforum@unime.it